

This is the accepted manuscript made available via CHORUS. The article has been published as:

## Sub-Coulomb $^3\text{He}$ transfer and its use to extract three-particle asymptotic normalization coefficients

M. L. Avila, L. T. Baby, J. Belarge, N. Keeley, K. W. Kemper, E. Koshchiy, A. N. Kuchera, G. V. Rogachev, K. Rusek, and D. Santiago-Gonzalez

Phys. Rev. C **97**, 014313 — Published 22 January 2018

DOI: [10.1103/PhysRevC.97.014313](https://doi.org/10.1103/PhysRevC.97.014313)

# Sub-Coulomb $^3\text{He}$ transfer and its use to extract three-particle asymptotic normalization coefficients

M. L. Avila,<sup>1,2</sup> L. T. Baby,<sup>2</sup> J. Belarge,<sup>2,\*</sup> N. Keeley,<sup>3</sup> K. W. Kemper,<sup>2</sup> E. Koshchiy,<sup>4</sup>  
A. N. Kuchera,<sup>2,†</sup> G. V. Rogachev,<sup>4</sup> K. Rusek,<sup>5</sup> and D. Santiago-Gonzalez<sup>2,‡</sup>

<sup>1</sup>*Physics Division, Argonne National Laboratory, Argonne, Illinois 60439, USA*

<sup>2</sup>*Department of Physics, Florida State University, Tallahassee, Florida 32306, USA*

<sup>3</sup>*National Centre for Nuclear Research,*

*ul. Andrzeja Soltana 7, 05-400 Otwock, Poland*

<sup>4</sup>*Department of Physics and Astronomy and Cyclotron Institute,*

*Texas A & M University, College Station, Texas 77843, USA*

<sup>5</sup>*Heavy Ion Laboratory, University of Warsaw,*

*ul. Pasteura 5a, 02-093, Warsaw, Poland*

## Abstract

Data for the  $^{13}\text{C}(^6\text{Li},t)^{16}\text{O}$  reaction, obtained in inverse kinematics at a  $^{13}\text{C}$  incident energy of 7.72 MeV, are presented. A distorted wave Born approximation (DWBA) analysis was used to extract spectroscopic factors and asymptotic normalization coefficients (ANCs) for the  $\langle ^{16}\text{O} | ^{13}\text{C} + ^3\text{He} \rangle$  overlaps, subject to the assumption of a fixed  $\langle ^6\text{Li} | ^3\text{He} + ^3\text{H} \rangle$  overlap. The variation of the extracted spectroscopic factors and ANCs as a function of various inputs to the DWBA calculations was explored. The extracted ANCs were found to vary as a cubic function of the radius of the potential well binding the transferred  $^3\text{He}$  to the  $^{13}\text{C}$  core while the spectroscopic factors varied as a quartic function of the radius. The ANC values could be determined to within a factor of two for this system.

---

\* J. Belarge is currently an MIT Lincoln Laboratory employee. No Laboratory funding or resources were used to produce the result/findings reported in this publication.

† Department of Physics, Davidson College, Davidson, North Carolina, 28035 USA

‡ Department of Physics and Astronomy, Louisiana State University, Baton Rouge, Louisiana 70803, USA

## I. INTRODUCTION

The use of the sub-Coulomb  $^{12}\text{C}(^6\text{Li},d)$   $\alpha$ -transfer reaction to extract reduced  $\alpha$ -particle widths was studied by Brune *et al.* [1]. Their work clearly demonstrated that reliable asymptotic normalization coefficients (ANCs) could be extracted from these measurements since they were insensitive to the details of the reaction if they were truly sub-Coulomb. The extracted values for the  $E2$   $S$  factors were consistent with previous results but had much reduced uncertainties. A further benchmark of this technique for determining ANCs was reported by Avila *et al.* [2] who used the sub-Coulomb  $^6\text{Li}(^{16}\text{O},d)$   $\alpha$ -particle transfer reaction to extract the partial  $\alpha$ -particle width for the 5.79 MeV  $1^-$  state in  $^{20}\text{Ne}$ , which was found to be in good agreement with the accepted value. This same group more recently used the sub-Coulomb  $^6\text{Li}(^{13}\text{C},d)$   $\alpha$ -particle transfer reaction to extract the Coulomb-modified ANC for the near-threshold  $^{17}\text{O}$   $1/2^+$  state at 6.356 MeV which can enhance the cross section for the  $^{13}\text{C}(\alpha,n)$  reaction at low energies [3]. This latter work was a remeasurement of this reaction carried out to understand the difference between the ANC for this state extracted from an earlier sub-Coulomb study [4] and the values derived from above-barrier studies. The difference was shown in Ref. [3] to be due to the extreme sensitivity of the measured cross section to changes in the bombarding energy that occurred during the run because of changes in target conditions.

While the main focus of Ref. [3] was on extracting  $\alpha$ -particle yields, the experimental system made it possible also to extract cross sections for the  $^6\text{Li}(^{13}\text{C},t)$  reaction to the first four excited states in  $^{16}\text{O}$ . The present work makes use of these cross sections to study the possible determination of both absolute spectroscopic factors and ANCs using this three-particle transfer reaction. It was shown in an early  $^{13}\text{C}(^6\text{Li},t)$  work [5] that this reaction strongly populated states in  $^{16}\text{O}$  that were different from those seen with the  $^{12}\text{C}(^6\text{Li},d)$  reaction and it was proposed that the  $(^6\text{Li},t)$  reaction could be used to probe quite different cluster configurations [6]. It was further shown that it was possible to extract mirror states in nuclei with the  $^{16}\text{O}(^6\text{Li},t/^3\text{He})$  reaction because of its selectivity [7]. However, there was considerable variation in the absolute values of the spectroscopic factors obtained because of the sensitivity of the calculated theoretical cross sections to the various input parameters [8], although as seen in Ref. [7], the relative strengths between mirror states were consistent. A later theoretical analysis [9] that compared the  $^{40}\text{Ca}(\alpha,n)$  reaction with  $^{40}\text{Ca}(^6\text{Li},t)$

reached the conclusion that  $({}^6\text{Li},t)$  was more reliable in determining three-particle structure information but was still plagued by the reaction uncertainties.

New low-energy data for the  ${}^6\text{Li}({}^{13}\text{C},t)$  reaction are presented in this work along with an extensive study of the extraction of spectroscopic factors and ANCs and their dependencies on the various parameters that go into their determination. In particular, while the entrance channel bombarding energy is sub-Coulomb, the reaction  $Q$ -value makes the exit tritons for the  ${}^{16}\text{O}$  states in question at or slightly above it so that the dependence on the exit channel optical potential parameters can be explored. In addition, the present work explores a case where the cluster components of the  ${}^6\text{Li}$  are tightly bound ( $\sim 16$  MeV), in contrast to the previous  $({}^6\text{Li},d)$  work.

## II. EXPERIMENT

Details of the experiment may be found in Ref. [3] and only a brief summary will be given here. An 8 MeV  ${}^{13}\text{C}$  beam was provided by the tandem van de Graaff accelerator of the Florida State University John D. Fox Accelerator Laboratory. Two  $\Delta E$ - $E$  counter telescopes were used, each constructed of four pin diode silicon detectors and one position sensitive proportional counter wire, which gave clear separation between the deuteron and triton reaction products, as seen in Fig. 1 which also shows a typical selection gate drawn around the triton group (solid lines). Figure 2 displays the triton spectrum and as can be seen the yields for the 6.92 MeV  $2^+$  and 7.12 MeV  $1^-$  states are easily extracted whereas those for the 6.05 MeV  $0^+$  and 6.13 MeV  $3^-$  states require peak fitting. The most important realization during the experiment was the need to change targets whenever any hint of contaminant build-up, which increased the target thickness, became apparent. This was manifest as a slight shift in the energy of the  ${}^6\text{Li}$  scattering peak to lower values over time. As described in Ref. [3], the target thickness was measured using  ${}^6\text{Li}$  recoils ejected from the target at forward angles in the laboratory reference frame by elastic scattering of an 8 MeV  ${}^{13}\text{C}$  beam and a 10 MeV  ${}^{16}\text{O}$  beam. Two different beams were employed to evaluate the systematic uncertainty of the target thickness measurements, found to be 10%. Elastic scattering of  ${}^6\text{Li}$  was also used to monitor target integrity and effective thickness.

Control measurements were performed when a new target was used for the first time and after about three hours of use; it was found that after 3 to 5 hours of target usage

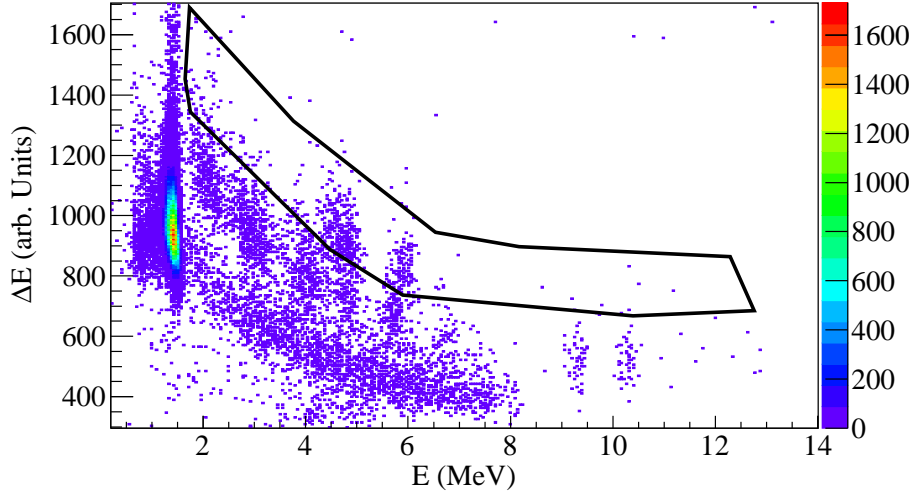


FIG. 1. (Color online)  $\Delta E$  vs.  $E$  two-dimensional scatter plot for a pin detector at  $30^\circ$  in the laboratory reference frame used for particle identification. A typical triton selection gate is shown by the solid lines.

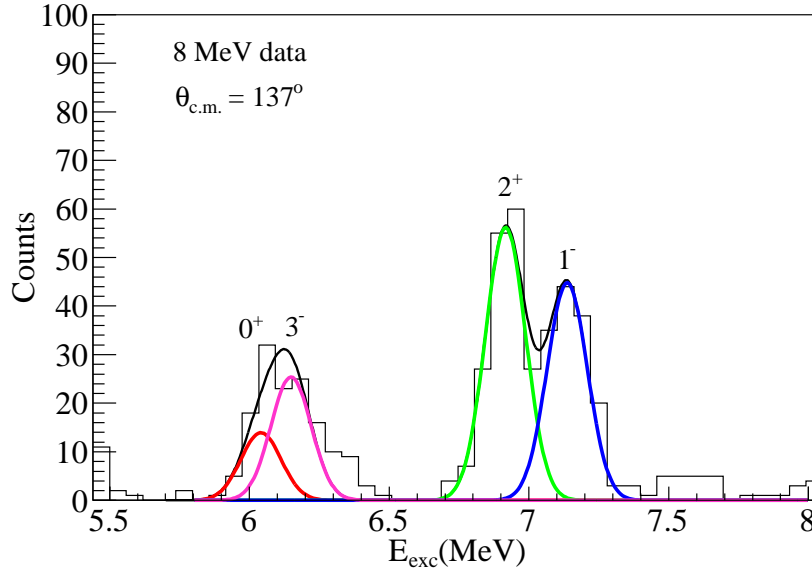


FIG. 2. (Color online) Spectrum of tritons from the  $^{13}\text{C}(^6\text{Li},t)^{16}\text{O}$  reaction at a triton scattering angle of  $137^\circ$  in the center of mass reference frame.

the energy of the elastically scattered  $^6\text{Li}$  had slightly reduced, attributed to contaminant build-up on the surface of the target (probably carbon or oxygen). Since sub-Coulomb cross sections are very sensitive to the incident energy, targets were changed every 3 to 5 hours and corresponding corrections implemented, see Refs. [2, 10] for full details. After the

correction due to the energy loss in the build-up material on the target, an effective energy of interaction of 7.72 MeV was calculated by taking into account the energy dependence of the cross section. This effective energy was calculated by integrating the cross section over the full target thickness and obtaining the value of the energy in the target at which one half of the yield was achieved, as explained in Ref. [11]. A beam energy of 7.72 MeV is therefore used in all the calculations presented in this work.

### III. DISTORTED WAVE BORN APPROXIMATION CALCULATIONS

A series of distorted wave Born Approximation (DWBA) calculations was carried out with the code FRESKO [12]. In order to reduce the number of variable parameters in these calculations we kept the wave function for the  $\langle {}^6\text{Li} \mid {}^3\text{He} + {}^3\text{H} \rangle$  overlap fixed. Following Ref. [13] the  ${}^3\text{He}$  was assumed to be bound to the  ${}^3\text{H}$  core in a pure  $2S$  state in a Woods-Saxon well of radius  $R = 2.60$  fm and diffuseness 0.60 fm with the depth adjusted to give the experimental binding energy, these parameters being such as to reproduce the wave function for the  ${}^3\text{He} + {}^3\text{H}$  relative motion displayed in Fig. 2 of Ref. [13]. The corresponding spectroscopic factor was 0.44, the average value determined in Ref. [13]. These parameters give a square ANC value for this overlap of  $C^2 = 359.89 \text{ fm}^{-1}$ .

For the  $\langle {}^{16}\text{O} \mid {}^{13}\text{C} + {}^3\text{He} \rangle$  overlaps we followed the procedure of Ref. [14], the  ${}^3\text{He}$  being bound to the  ${}^{13}\text{C}$  core in a Woods-Saxon well of radius  $R = 4.7$  fm (i.e.  $2.0 \times 13^{1/3}$  fm) and diffuseness  $a = 0.65$  fm, the well depth again being adjusted to give the correct binding energy for the particular  ${}^{16}\text{O}$  state (ranging from 16.74 MeV for the 6.05 MeV  $0^+$  state to 15.67 MeV for the 7.12 MeV  $1^-$  state). Since two different  $L$  values are allowed for the relative motion of the  ${}^3\text{He}$  relative to the  ${}^{13}\text{C}$  core for a given state in  ${}^{16}\text{O}$  we adopted the  $L$  values of Ref. [14] where it was found that the angular distributions could be well described by a single  $L$ -transfer for each state. We give the values of  $L$ , together with the number of nodes in the radial wave function,  $N$ , including that at  $r = 0$  but not that at  $r = \infty$ , in Table I.

For the main set of calculations we took the entrance channel  ${}^6\text{Li} + {}^{13}\text{C}$  optical potential parameters from Table II of Ref. [15] and the exit channel  ${}^3\text{H} + {}^{16}\text{O}$  parameters from Ref. [16]. The incident  ${}^{13}\text{C}$  energy is below the nominal Coulomb barrier for this system, so in principle the results should be independent of the choice of entrance channel optical

TABLE I. Number of nodes in the radial wave function,  $N$ , and relative angular momenta,  $L$ , of the  $^3\text{He}$  cluster relative to the  $^{13}\text{C}$  core for the  $^{16}\text{O}$  states studied here.

$E_{\text{ex}}$ (MeV)	$J^\pi$	$N$	$L$
6.05	$0^+$	3	1
6.13	$3^-$	2	2
6.92	$2^+$	3	1
7.12	$1^-$	2	2

potential. However, the reaction  $Q$  value is such (+7 MeV) that the  $^3\text{H}$  ejectiles are above the respective Coulomb barrier so some sensitivity to the choice of optical potential in the exit channel is to be expected. This is in contrast to the studies of Refs. [2] and [3] where, due to the significantly less positive reaction  $Q$  values, the  $^2\text{H}$  ejectiles for the states of interest are below the respective exit channel Coulomb barriers.

A set of fits to the transfer angular distributions was obtained based on these inputs. Calculations were performed with the full (Coulomb + nuclear) optical potentials in both entrance and exit channels, Coulomb potential only in the entrance channel plus full optical potential in the exit channel, full optical potential in the entrance channel plus Coulomb potential only in the exit channel, and finally Coulomb potential only in both entrance and exit channels. The searching version of the FRESKO code, SFRESKO, was used to obtain the best fit in each case by varying the spectroscopic factor to obtain the minimum value of  $\chi^2$ . Given the relatively large uncertainties in the experimental data this method of defining the best fit should give more objective results. All calculations employed the post form of the DWBA and included the full complex remnant term (calculations using the prior form gave identical results).

The DWBA angular distributions are compared with the data in Fig. 3. It can be seen from Fig. 3 that there is considerable sensitivity of the shape of the transfer angular distributions to the presence of a nuclear component in the entrance channel distorting potential as well as in the exit channel. The values obtained for the ANCs are also sensitive to the presence of nuclear potentials in both exit and entrance channels, as Table II shows. Here, although the effect of omitting the nuclear part of the entrance channel distorting potential is by no means negligible—a reduction by a factor of about 1.5 in the  $\text{ANC}^2$ —

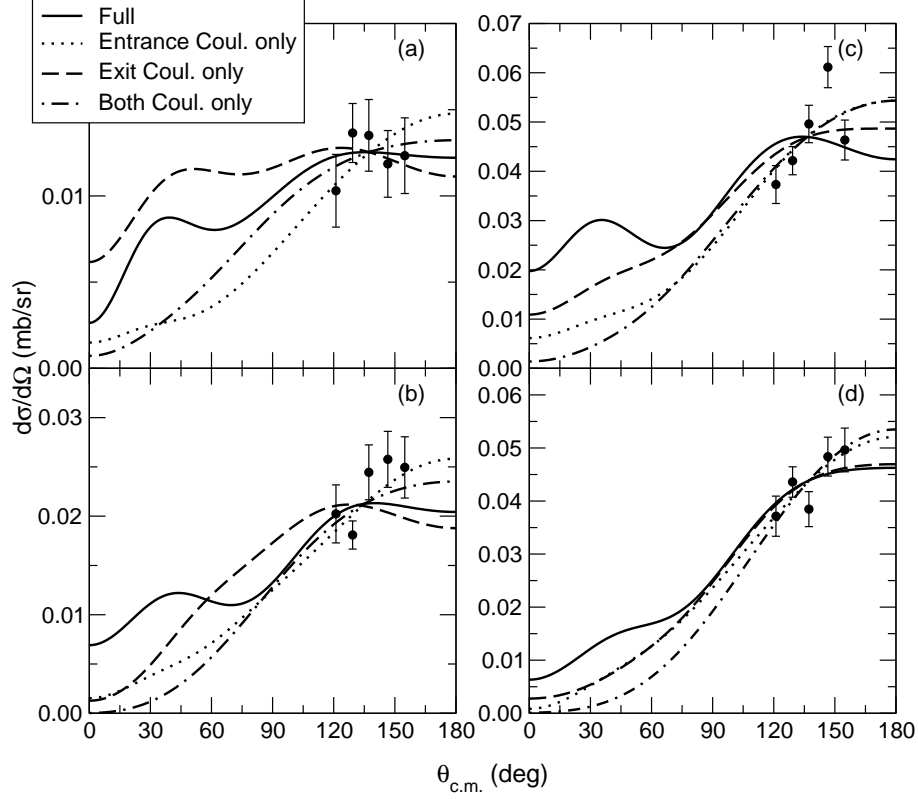


FIG. 3. Angular distributions for the  $^{13}\text{C}(^6\text{Li},t)^{16}\text{O}$  reaction to: (a) the 6.05 MeV  $0^+$  state, (b) the 6.13 MeV  $3^-$  state, (c) the 6.92 MeV  $2^+$  state and (d) the 7.12 MeV  $1^-$  state. The solid curves denote the results of calculations using the full (nuclear plus Coulomb) distorting potentials in both entrance and exit channels, the dotted curves calculations using the full potential in the exit channel but only the Coulomb potential in the entrance channel, the dashed curves calculations using the full potential in the entrance channel but only the Coulomb potential in the exit channel and the dot-dashed curves calculations using only the Coulomb potential in both entrance and exit channels.

the main effect comes from the omission of the nuclear part of the exit channel distorting potential.

Having established that the DWBA calculations are sensitive to the presence of a nuclear component in the distorting potentials, especially in the exit channel, the dependence on the choice of the nuclear potential itself was investigated. This was done by performing calculations using global parameter sets, that of Cook [17] for the  $^6\text{Li} + ^{13}\text{C}$  potential and that of Pang *et al.* [18] for the  $^3\text{H} + ^{16}\text{O}$  potential, the latter being adapted for targets in the  $1p$  shell. One set of calculations using the global parameters in both entrance and exit



TABLE II. Square ANCs (in  $\text{fm}^{-1}$ ) obtained from the DWBA fits to the data for the various cases with and without nuclear components of the distorting potentials in the entrance and exit channels. The  $\chi^2/N$  for each fit are also given, where  $N$  is the number of data points.

Case	$0^+$		$3^-$		$2^+$		$1^-$	
	ANC <sup>2</sup>	$\chi^2/N$	ANC <sup>2</sup>	$\chi^2/N$	ANC <sup>2</sup>	$\chi^2/N$	ANC <sup>2</sup>	$\chi^2/N$
Full	$9.12 \times 10^6$	0.34	$1.52 \times 10^6$	1.90	$4.76 \times 10^6$	4.20	$5.71 \times 10^6$	1.01
Coulomb only entrance	$5.90 \times 10^6$	0.55	$0.98 \times 10^6$	0.86	$3.39 \times 10^6$	2.11	$3.96 \times 10^6$	0.75
Coulomb only exit	$2.01 \times 10^6$	0.39	$0.34 \times 10^6$	2.53	$1.09 \times 10^6$	2.94	$1.52 \times 10^6$	0.94
Coulomb only both	$1.74 \times 10^6$	0.35	$0.30 \times 10^6$	1.21	$1.04 \times 10^6$	2.19	$1.42 \times 10^6$	0.84

TABLE III. Square ANCs (in  $\text{fm}^{-1}$ ) obtained from the DWBA fits to the data for various choices of entrance and exit channel distorting potentials, see text for details. The first row is repeated from Table II (row 1) for ease of reference. The  $\chi^2/N$  for each fit are also given, where  $N$  is the number of data points.

Potentials	$0^+$		$3^-$		$2^+$		$1^-$	
	ANC <sup>2</sup>	$\chi^2/N$	ANC <sup>2</sup>	$\chi^2/N$	ANC <sup>2</sup>	$\chi^2/N$	ANC <sup>2</sup>	$\chi^2/N$
Fit	$9.12 \times 10^6$	0.34	$1.52 \times 10^6$	1.90	$4.76 \times 10^6$	4.20	$5.71 \times 10^6$	1.01
Global both	$19.49 \times 10^6$	0.43	$3.61 \times 10^6$	1.37	$10.80 \times 10^6$	2.40	$13.37 \times 10^6$	0.84
Global exit	$11.71 \times 10^6$	0.39	$2.07 \times 10^6$	2.10	$6.60 \times 10^6$	2.75	$8.21 \times 10^6$	1.06

channels and one set using the potential of Ref. [15] in the entrance channel and the global potential of Ref. [18] in the exit channel were performed. The spectroscopic factors were again fitted to the data by minimizing  $\chi^2$  with SFRESCO.

The angular distributions are plotted on Fig. 4 and the ANCs obtained given in Table III. In both cases we repeat the results obtained with the empirical optical model potentials in both entrance and exit channels (labeled as “fit” on Fig. 4) for ease of reference. The shapes of the transfer angular distributions are slightly better reproduced when the global parameters are used to calculate both the entrance and exit channel distorting potentials although without the necessary elastic scattering data it is impossible to say which calculation is more in keeping with the underlying assumptions of the DWBA (i.e. that the

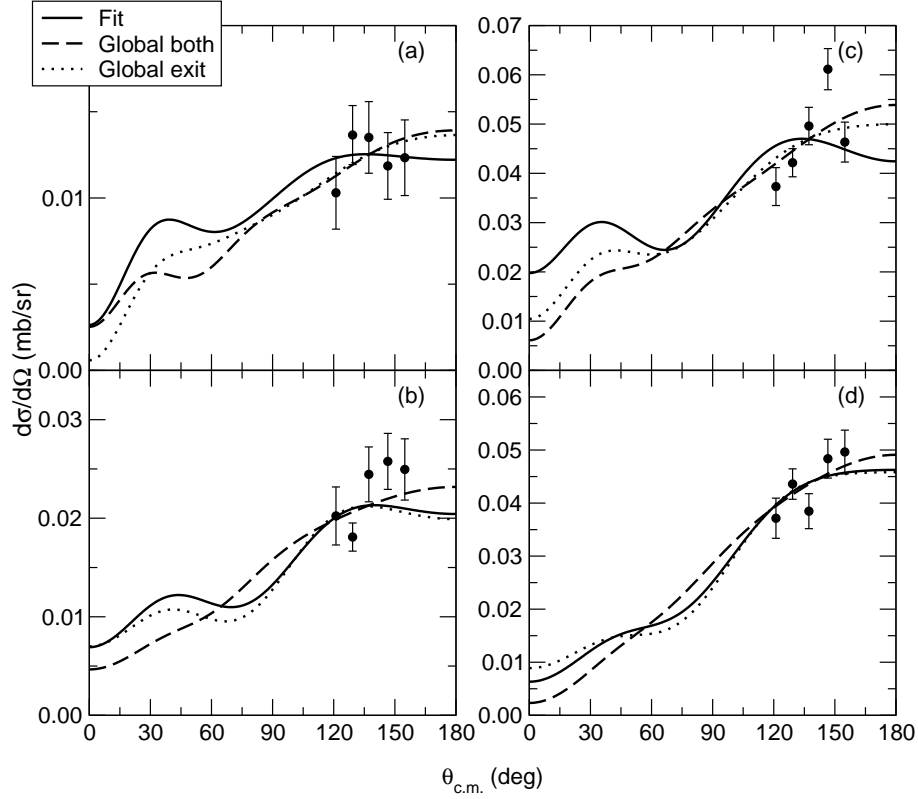


FIG. 4. Angular distributions for the  $^{13}\text{C}(^6\text{Li},t)^{16}\text{O}$  reaction to: (a) the 6.05 MeV  $0^+$  state, (b) the 6.13 MeV  $3^-$  state, (c) the 6.92 MeV  $2^+$  state, and (d) the 7.12 MeV  $1^-$  state. The dashed and dotted curves denote DWBA fits with distorting potentials calculated using global parameter sets in both entrance and exit channels and the exit channel only, respectively. The solid curves denote DWBA fits with entrance and exit channel distorting potentials taken from Refs. [15] and [16], respectively, repeated from Fig. 3.

distorting potentials should reproduce the appropriate elastic scattering data). More importantly, Table III shows that the use of global parameters in both entrance and exit channels increases the extracted  $\text{ANC}^2$  values by factors of just over two for all states, demonstrating a significant dependence on the choice of the distorting potentials even at this low incident energy. Narrowing the choice of acceptable distorting potentials would require data over a larger angular range and of much increased precision; given the small cross sections involved this represents a considerable experimental challenge.

Having tested the sensitivity to the choice of the distorting potentials we now turn to the parameters of the potential binding the transferred  $^3\text{He}$  to the  $^{13}\text{C}$  core. The choice of the radius and diffuseness parameters is somewhat arbitrary in the absence of constraints

from other sources if the usual well-depth prescription is employed (it should be recalled that the depth of the binding potential well is arranged to give the experimental binding energy in this approximation). The choice of binding potential radius is perhaps the largest single source of uncertainty in the extraction of absolute spectroscopic factors from fits to angular distribution data (the dependence on the diffuseness is usually less important). Absolute values of  $\alpha$ -particle spectroscopic factors obtained in this way often vary by factors of five or more over a “reasonable” range of binding potential radii. However, it has been demonstrated in many cases that the ANCs are much less sensitive to the choice of binding potential parameters, with little or no significant variation over quite large ranges of binding potential radius.

In order to test the sensitivity of both the absolute spectroscopic factors and the ANCs extracted from the DWBA fits to the choice of binding potential radius we carried out a series of tests where the  $r_0$  value ( $R = r_0 \times 13^{1/3}$  fm) was varied from 1.5 to 2.5 fm, i.e. a range of  $\pm 0.5$  fm from the value used in the main analyses. For these tests we used the same distorting potentials as in the calculations labeled “Fit” in Table III in both entrance and exit channels, i.e. those of Refs. [15] and [16], respectively. We plot the resulting spectroscopic factor and  $\text{ANC}^2$  values as a function of  $r_0$  in Fig. 5.

The first thing to note from Fig. 5 is that the variations in both the spectroscopic factors and the ANCs over the wide range of  $r_0$  values explored are large, the changes in spectroscopic factor over the whole range amounting to factors of 41, 60, 39, and 59 and in  $\text{ANC}^2$  to factors of 4.5, 3.9, 4.2, and 3.3 for the  $0^+$ ,  $3^-$ ,  $2^+$  and  $1^-$  states, respectively. The spectroscopic factors vary as quartic functions of  $r_0$  whereas the ANCs vary as cubic functions. However, it is clear that the ANC values are much less sensitive to the choice of  $r_0$  than the corresponding spectroscopic factors, the total change being approximately an order of magnitude smaller. The extent of the uncertainty in the ANCs will of course depend considerably on the range of the variation in  $r_0$  it is considered reasonable to take. In this particular case the  $\chi^2$  values do not help us since the variation in  $\chi^2$  due to making different choices of  $r_0$  was considerably smaller for all the states considered than that caused by using global optical parameters to calculate the entrance and exit channel distorting potentials in lieu of the empirical potentials, making it impossible to narrow the “acceptable” range of  $r_0$  by this criterion with the existing data. However, if the angular distributions could be measured to a precision of  $\pm 10\%$  over a much wider angular range it should be possible to

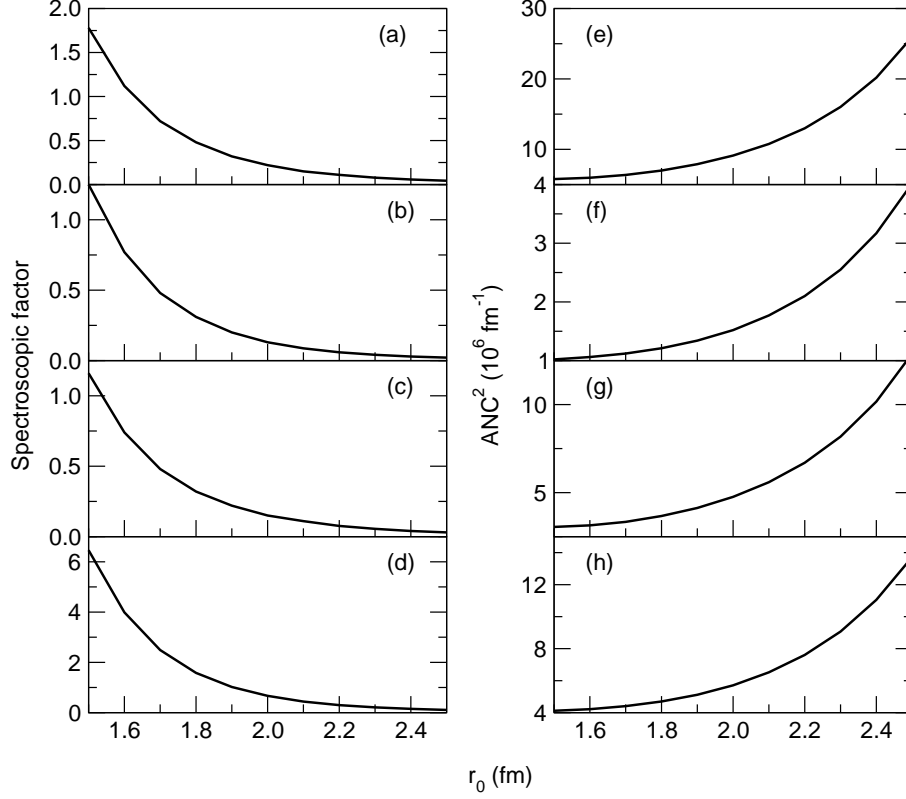


FIG. 5. Spectroscopic factor and  $ANC^2$  values for the  $\langle {}^{16}\text{O} | {}^{13}\text{C} + {}^3\text{He} \rangle$  overlaps to: (a), (e) the 6.05 MeV  $0^+$  state; (b), (f) the 6.13 MeV  $3^-$  state; (c), (g) the 6.92 MeV  $2^+$  state; (d), (h) the 7.12 MeV  $1^-$  state as a function of  $r_0$ . See text for details.

rule out some of the smaller  $r_0$  values since the shapes of the calculated angular distributions do differ enough for these cases at angles  $\theta_{\text{c.m.}} < 90^\circ$  to make this feasible.

#### IV. SUMMARY AND CONCLUSIONS

New data for the  ${}^{13}\text{C}({}^6\text{Li}, t){}^{16}\text{O}$  reaction taken in inverse kinematics at an incident  ${}^{13}\text{C}$  energy of 7.72 MeV were reported. The incident energy is sufficiently low that the entrance channel is below the nominal Coulomb barrier while the reaction  $Q$  value is such that the  ${}^3\text{H}$  ejectiles are above their respective barrier. It might therefore *a priori* be expected that the results of DWBA calculations would be insensitive to the nuclear part of the entrance channel distorting potential, although some sensitivity to the choice of exit channel potential was probable. However, while the results were in fact also sensitive to the nuclear part of the entrance channel potential as well as the exit channel potential, it was possible to determine

the extracted ANC's to within a factor of just over two for the cases examined here.

The dependence of the extracted ANC's on the choice of binding potential radius was also investigated and it was found that they vary as a cubic function of  $r_0$ . While this variation is much smaller than that of the corresponding spectroscopic factors (which vary as a quartic function of  $r_0$ ) it is still significant. The change in  $\chi^2$  of the fit to the data does not help establish a “reasonable” range of  $r_0$  values in this case since it is smaller than that caused by different choices of distorting potentials. Therefore, the contribution to the overall uncertainty of the extracted ANC's due to this source will depend very much on what is considered to be a reasonable variation in  $r_0$ . The importance of additional information about the bound state well potential in extracting reduced normalization factors was already emphasized by Rapaport and Kerman in their early study of sub-Coulomb ( $d,p$ ) reactions [19].

Finally, as pointed out in Ref. [3], at sub-Coulomb incident energies special care must be taken to avoid build-up of contaminants on the surface of the target, which will reduce the effective beam energy. In the sub-Coulomb barrier regime the cross sections are varying most rapidly as a function of incident energy, so a relatively small change can have significant consequences, as discussed in Ref. [3].

Our conclusions are as follows. It was demonstrated that even at a nominally sub-barrier incident energy the spectroscopic factors and ANC's extracted from fits to angular distribution data for the  $^{13}\text{C}(^6\text{Li},t)^{16}\text{O}$  reaction had a significant dependence on the choice of the distorting potentials in both entrance and exit channels. Thus, even at such low incident energies, it can be worthwhile checking whether the elastic scattering is true Rutherford over the whole angular range (within experimental uncertainties) in order to be sure that the analysis will be independent of the choice of nuclear distorting potential, at least in the entrance channel. While the angular distributions predicted by the two sets of  $^6\text{Li} + ^{13}\text{C}$  optical potential parameters tested here, those of Poling *et al.* [15] and Cook [17], both deviate only slightly from Rutherford scattering (ratio to Rutherford at  $180^\circ$  of 0.91 and 0.85, respectively) this is sufficient for them to have a significant influence on the DWBA calculations in this particular case.

While the variation of the extracted ANC's as a function of the radius of the potential well binding the transferred  $^3\text{He}$  to the  $^{13}\text{C}$  core was much slower than that of the corresponding spectroscopic factors it was still significant. It is possible that this could be linked to the

much larger binding energy of the  ${}^3\text{He} + {}^3\text{H}$  clusters in  ${}^6\text{Li}$  compared to that of the  ${}^4\text{He} + {}^2\text{H}$  clusters of previous ( ${}^6\text{Li}, d$ ) studies, e.g. [2, 3]. This leads to a considerably less extended relative motion wave function, cf. Fig. 2 of Ref. [13]. Similar considerations will apply to the  $\langle {}^{16}\text{O} \mid {}^{13}\text{C} + {}^3\text{He} \rangle$  wave functions. However, a test of this hypothesis would require a comparative study of a large number of cases and is beyond the scope of the current investigation. The changes in  $\chi^2$  for the best fit for a particular choice of  $r_0$  were not large enough (being smaller than those due to different choices of distorting potentials) to help provide a constraint on a “reasonable” range of  $r_0$  values, possibly due to the structureless nature of the angular distributions, a feature of sub-barrier transfer reactions. Therefore, under these conditions it may be necessary to provide constraints on the acceptable range of  $r_0$  values from other considerations, such as the rms radii of the bound state wave functions obtained from structure calculations, in order to provide a better estimate of the uncertainty in the ANC since the maximum likelihood technique, as used e.g. by Pellegriti *et al.* [20], could well allow unphysical values of  $R$  based as it is on goodness of fit alone. If the angular range of the measurement could be extended to cover angles  $\theta_{\text{c.m.}} < 90^\circ$  at a precision of  $\pm 10\%$  it should be possible to narrow the range of acceptable  $r_0$  values somewhat, due to the dependence of the shape of the calculated angular distributions on  $r_0$ , but only at the lower end.

## ACKNOWLEDGMENTS

The authors acknowledge the financial support provided by the National Science Foundation (USA) under Grant No. PHY-456463. M.L.A. acknowledges that this material is based upon work supported by the U.S. Department of Energy, Office of Science, Office of Nuclear Physics, under contract number DE-AC02-06CH11357. G.V.R. and E.K. acknowledge that this material is based upon their work supported by the U.S. Department of Energy, Office of Science, Office of Nuclear Science, under Award No. DE-FG02-93ER40773. G.V.R. also acknowledges the financial support of the Welch Foundation (USA) (Grant No. A-1853).

---

[1] C. R. Brune, W. H. Geist, R. W. Kavanagh, and K. D. Veal, Phys. Rev. Lett. **83**, 4025 (1999).

- [2] M. L. Avila, G. V. Rogachev, E. Koshchiy, L. T. Baby, J. Belarge, K. W. Kemper, A. N. Kuchera, and D. Santiago-Gonzalez, Phys. Rev. C **90**, 042801(R) (2014).
- [3] M. L. Avila, G. V. Rogachev, E. Koshchiy, L. T. Baby, J. Belarge, K. W. Kemper, A. N. Kuchera and D. Santiago-Gonzalez, Phys. Rev. C **91**, 048801 (2015).
- [4] E. D. Johnson, G. V. Rogachev, A. M. Mukhamedzhanov, L. T. Baby, S. Brown, W. T. Cluff, A. M. Crisp, E. Diffenderfer, V. Z. Goldberg, B. W. Green, T. Hinnners, C. R. Hoffman, K. W. Kemper, O. Momotyuk, P. Peplowski, A. Pipidis, R. Reynolds, and B. T. Roeder, Phys. Rev. Lett. **97**, 192701 (2006).
- [5] G. Bassani, T. H. Kruse, N. Saunier, and G. Souchere, Phys. Lett. B **30**, 621 (1969).
- [6] A. D. Panagiotou and H. E. Gove, Nucl. Phys. A **196**, 145 (1972); R. A. Lindgren, H. H. Gutbrod, H. W. Fulbright and R. G. Markham, Phys. Rev. Lett. **29**, 798 (1972).
- [7] H. G. Bingham, H. T. Fortune, J. D. Garrett, and R. Middleton, Phys. Rev. Lett. **26**, 1448 (1971); J. D. Garrett, H. G. Bingham, H. T. Fortune, and R. Middleton, Phys. Rev. C **5**, 682 (1972).
- [8] A. Cunsolo, A. Foti, G. Immè, G. Pappalardo, G. Raciti, F. Rizzo, and N. Saunier, Phys. Rev. C **21**, 952 (1980).
- [9] J. J. Hamill and P. D. Kunz, Phys. Lett. B **129**, 5 (1983).
- [10] M. L. Avila, Ph.D. thesis, Florida State University, 2013 (unpublished).
- [11] C. E. Rolfs and W. S. Rodney, *Cauldrons in the Cosmos: Nuclear Astrophysics* (University of Chicago Press, Chicago, 1988), Vol. 1.
- [12] I. J. Thompson, Comput. Phys. Rep. **7**, 167 (1988).
- [13] M. F. Werby, M. B. Greenfield, K. W. Kemper, D. L. McShan, and S. Edwards, Phys. Rev. C **8**, 106 (1973).
- [14] K. Abdo, L. Dennis, A. Frawley, and K. W. Kemper, Nucl. Phys. A **377**, 281 (1982).
- [15] J. E. Poling, E. Norbeck, and R. R. Carlson, Phys. Rev. C **13**, 648 (1976).
- [16] D. J. Pullen, J. R. Rook, and R. Middleton, Nucl. Phys. **51**, 88 (1964).
- [17] J. Cook, Nucl. Phys. A **388**, 153 (1982).
- [18] D. Y. Pang, W. M. Dean, and A. M. Mukhamedzhanov, Phys. Rev. C **91**, 024611 (2015).
- [19] J. Rapaport and A. Kerman, Nucl. Phys. A **119**, 641 (1968).
- [20] M. G. Pellegriti, F. Hammache, P. Roussel, L. Audouin, D. Beaumel, P. Descouvemont, S. Fortier, L. Gaudefroy, J. Kiener, A. Lefebvre-Schuhl, M. Stanoiu, V. Tatischeff, and M. Vilmay,

Phys. Rev. C **77**, 042801(R) (2008).